Impact of ultrasound frequency on the corrosion resistance of electroless nickel-phosphorus-nanodiamond plating

Habib Ashassi-Sorkhabi [a,*], Amir Kazempour, Jafar Mostafaei, Elnaz Asghari

Electrochemistry Research Laboratory, Department of Physical Chemistry, Faculty of Chemistry, University of Tabriz, Tabriz, Iran

ARTICLE INFO

ABSTRACT

The nickel-phosphorus (Ni-P) and nickel-phosphorus-nanodiamond (Ni-P-ND) coatings were deposited on mild steel via electroless plating without ultrasound and under ultrasonic agitation with different frequencies of 25, 50, 75, 100, and 150 kHz. The as-prepared coatings were characterized using scanning electron microscopy (SEM), energy-dispersive X-ray spectroscopy (EDX), and X-ray diffraction (XRD). The corrosion performance of the fabricated layers was evaluated in 3.5 wt% NaCl solution by electrochemical impedance spectroscopy (EIS) and potentiodynamic polarization. Results of the corrosion tests demonstrated that deposition under ultrasonic power provided coatings with higher stability in the corrosive environment. The corrosion rate decreased with increasing ultrasound frequency from 25 to 75 kHz but increased with further increase in frequency. This introduced 75 kHz as the optimum ultrasound frequency for electroless plating of Ni-P. It was also observed that the corrosion resistance of the proposed coating was improved through the incorporation of 40 ppm nanodiamond into the Ni-P matrix.

1. Introduction

Electroless nickel-phosphorus (Ni-P) coatings are broadly applied to various metallic substrates to modify their surface properties, such as electrochemical behavior and hardness. This type of coating is frequently used in multiple fields, including chemical electronics, aerospace, mechanical, and oil-gas industries [1–7]. It has been reported that Ni-P coatings express practical anti-corrosion features, wear resistance, uniformity of deposit, and high abrasion [8,9]. Thanks to such characteristics, Ni-P films could provide an efficient protective barrier for different metals, particularly steel alloys as one of the most used metals in the industry [10–15]. Because of the cathodic nature of this coating towards steel substrate, the risk of developing galvanic cells with a large cathode-to-anode area ratio at the cracks of the coating should be taken into account [16]. It is known that the addition of particles, especially nanoparticles, to the Ni-P matrix enhances the characteristics of the surface, depending on the nature of the additive [17–19]. Within this

framework, various nanoparticles such as Si_3N_4 [12], SiC [20], graphene [21], MOF [22], and ZrO_2 [23] have recently been reported to improve the corrosion and wear resistance of the Ni-P coating. It is believed that the presence of nanoparticles provides nanocomposite coatings with fewer cracks and porosity, resulting in improved corrosion protection. Moreover, ultrasound-assisted electrodeposition of Ni coatings has been proposed because of advantages like increased deposition rate and reduced internal stress of the resulting coating [24–26]. In this regard, many works have been carried out on the ultrasonically prepared Ni-P coatings on different types of substrates. However, the number of reports on the influence of ultrasound power frequency is limited. On this basis, the present work provides a systematic study on the electroless deposition of Ni-P and Ni-P-nanodiamond (Ni-P-ND) coatings under ultrasound waves imposed in a wide range of frequencies.

2. Experimental
2.1. Materials

* Corresponding author. e-mail: habib.ashassi@gmail.com

The main chemicals used in this work are nickel sulfate ($NiSO_4.6H_2O$), sodium hypophosphite (NaH_2PO_2), sodium acetate (CH_3COONa), lactic acid ($NaC_6H_3O_7$), thiourea (CH_4N_2S), tween 20 as a surfactant ($C_{58}H_{114}O_{26}$), nanodiamond (average size 4 nm), and sodium chloride (NaCl). Nanodiamond was purchased from Plasma Chem GmbH, and the rest of the materials were supplied from Merck.

2.2. Apparatus

The surface morphologies of the synthesized Ni-P and Ni-P-ND coatings were analyzed by TESCAN MIRA III scanning electron microscopy. The chemical compositions of the coatings were determined using an energy-dispersive X-ray spectroscopy (EDX) system attached to the SEM. The X-ray diffraction (XRD) patterns of the samples were prepared by a Siemens D5000 X-ray diffractometer. The microhardness of the coatings was measured using an HV-1000Z microhardness tester. The pH of the bath was adjusted by a Metrohm 654 pH meter, and the weightings were carried out by a Unimatic CLX40 balance. The ultrasonic probe used for the synthesis was Dr. Hielscher GmbH, up to 400 s. The electrochemical corrosion tests were performed using a PGSTAT30 Autolab.

2.3. Deposition of Ni-P and Ni-P-ND coatings

Before deposition, the mild steel samples with a surface area of 1×1 cm^2 were abraded by SiC papers with various grads from 200 to 2500 and then initially cleaned using distilled water. To remove any dirt or grease substance from the steel surface, the samples were immersed in hot 1 M NaOH solution for about 3 min and then washed with acetone and distilled water. Furthermore, the acid treatment of 30% HCl was proceeded for 1 min to remove oxide layers from the surface. Finally, the samples were rinsed with distilled water and immersed in the deposition bath containing 30 g·L^{-1} $NiSO_4.6H_2O$, 30 g·L^{-1} NaH_2PO_2, 45 g·L^{-1} CH_3COONa, 25 mL·L^{-1} $NaC_6H_3O_7$, 0.005 g·L^{-1} CH_4N_2S, and 0.003 g·L^{-1} tween 20. To prepare Ni-P-ND coatings, 40 ppm nanodiamond particles were added to the deposition bath. Ultrasonic waves from 0 to 150 kHz were imposed to the bath during 1 h electroless deposition. The bath temperature was kept constant at 88-90 ºC by a thermostat, and the pH of the bath was adjusted to 4.8 using dilute solutions of H_2SO_4 and NaOH.

*2.4. Electrochemical corrosion tests*

The corrosion resistance of the coated samples was investigated in 3.5% NaCl solution by electrochemical impedance spectroscopy (EIS) and potentiodynamic polarization (PDP) techniques. All the measurements were performed in a three-electrode cell containing a mounted mild steel coupon, a platinum wire, and an Ag/AgCl (saturated KCl) electrode as the working, counter, and reference electrodes, respectively. The EIS measurement was carried out in a frequency range from 10 kHz to 10 mHz with voltage perturbation amplitude of 10 mV. PDP curves were recorded in a potential range of -250 to 250 mV versus open circuit potential at a scan rate of 1 mV·s^{-1}.

3. Results and discussion

3.1. XRD patterns of the coatings

Fig. 1 depicts the XRD patterns of electroless plating of Ni-P and Ni-P-ND coatings under ultrasonic waves with a frequency of 75 kHz. A broad peak appeared at $2\Theta = 45º$ for both of the coatings is the characteristic peak of Ni-P coatings, indicating a typical semi-crystalline phase, which shows a mixture of crystallized and amorphous structures [1,27,28]. The amount of nanodiamond particles in the Ni-P layer is minimal. For this reason, its diffraction peak is not observable in the XRD pattern obtained. However, the elemental composition of the coatings obtained from EDS confirms the presence of ND particles in the deposited coating (see Fig. 2).
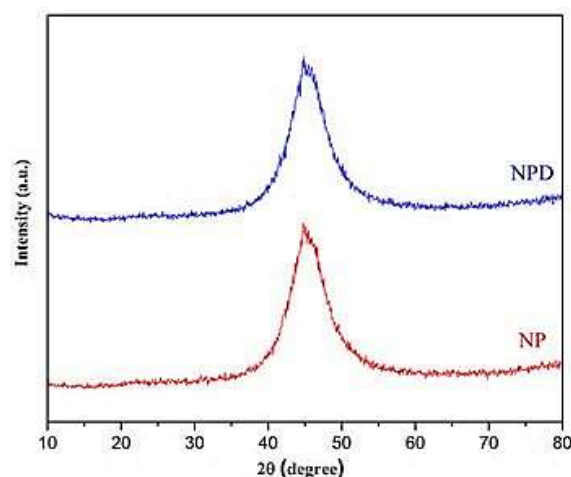

Figure 1. XRD patterns of the electroless Ni-P (determined as NP) and Ni-P-ND (determined as NPD) coatings produced under ultrasound wave with the frequency of 75 kHz.

3.2. SEM images and EDS analysis of the coatings

Fig. 2 shows the surface morphologies of the Ni-P and Ni-P-ND coatings synthesized under ultrasonic waves with a frequency of 75 kHz. Accordingly, the addition of ND particles has changed the coating morphology. The Ni-P-ND coating has a rough surface

and provides a nodular structure all over the surface. Such systems are formed because of the presence of ND particles, resulting in improved corrosion resistance of the coating.
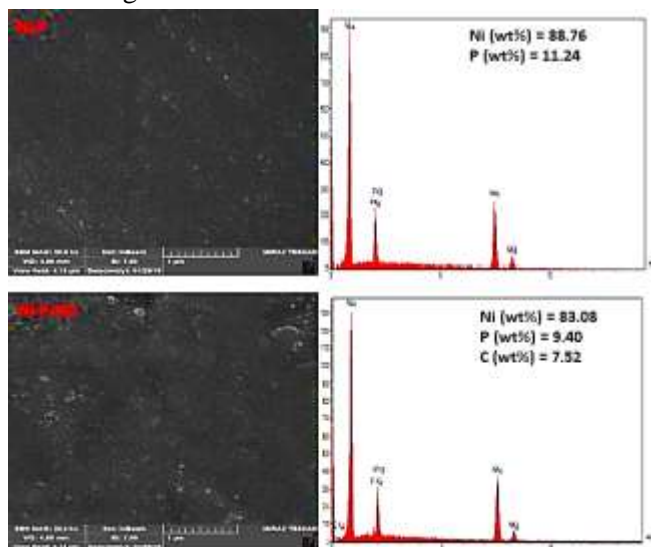

Figure 2. SEM and EDX analyses of the electroless Ni-P and Ni-P-ND coatings produced under ultrasound wave with the frequency of 75 kHz.

3.3. Corrosion properties of the prepared coatings
Improvements in corrosion resistance of the Ni-P coating as a result of imposing ultrasonic waves and the addition of ND particles were evaluated by the obtained EIS data. Fig. 3 illustrates the Nyquist diagrams for the two Ni-P and Ni-P-ND coatings deposited under ultrasonic waves with frequencies of 0, 25, 50, 75, 100, and 150 kHz. The resulted Nyquist plots had two time constants, which were fitted by the equivalent circuit shown in Fig. 4b. On this basis, the first time constant is attributed to the Ni-P coatings and is evidenced as a loop appearing at high frequencies in the Nyquist diagrams. This time constant includes R_{coat} and CPE_{cot}, which describe the coating resistance and constant phase element, respectively. The second time constant that appeared as a loop located at intermediate frequencies corresponds to the double-layer. This time constant is described by CPE_{dl}, which represents the double-layer constant phase element, and R_{corr}, which shows the steel corrosion resistance or charge transfer resistance of the metal. R_s is also determined as the solution resistance. The impedance parameters obtained from fitting the experimental EIS data are collected in Table 1. The deposition of Ni-P coating under any condition has significantly improved the corrosion resistance of the bare steel substrate. It is also evident that the incorporation of 40 ppm ND particles into

the coating increased in the corrosion protection of the Ni-P coating. This is due to the hard nature of ND particles, which could increase the hardness of the deposited coating.
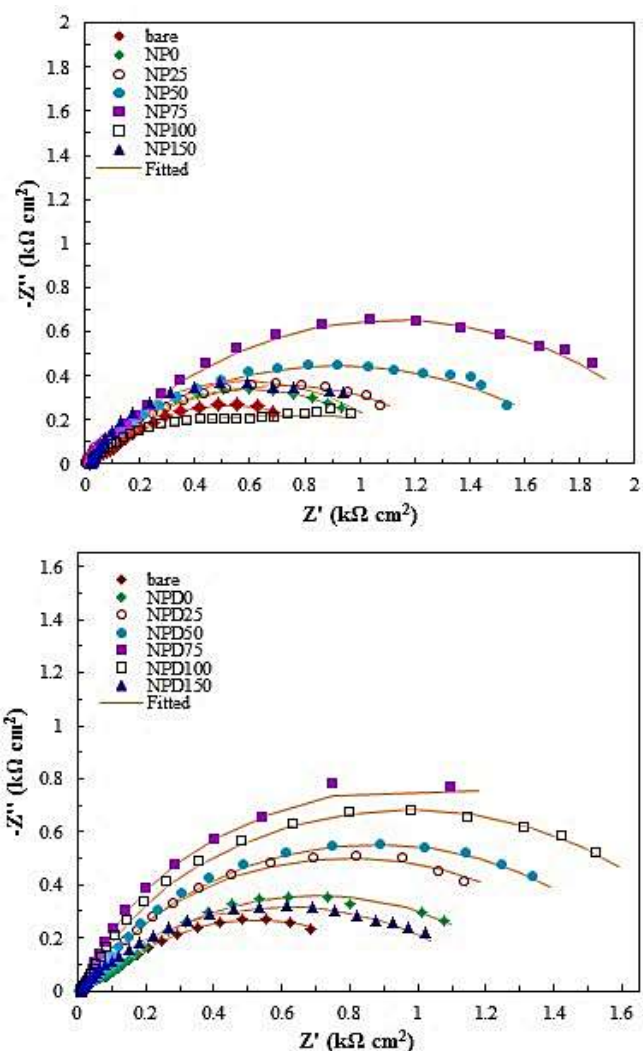
Figure 3. Nyquist diagrams of the electroless Ni-P (determined as NP) and Ni-P-ND (determined as NPD) coatings fabricated under ultrasound with various frequencies.
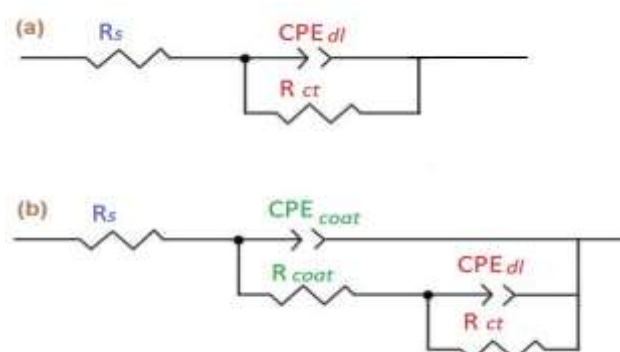
Figure 4. Equivalent circuits used for fitting the experimental Nyquist diagrams. Circuit (a) was employed for bare steel and circuit (b) was applied for coated samples.

Table 1. Electrochemical impedance parameters obtained for electroless Ni-P and Ni-P-ND coatings produced under ultrasound agitation with various frequencies.

| Sample | Ultrasound frequency (kHz) | CPE_{coat} | | R_{coat} (Ω cm^2) | CPE_{dl} | | R_{ct} (Ω cm^2) | R_p (Ω cm^2) | Fitting error |
		$Y_0 \times 10^{-5}$ (Ω^{-1}cm^{-2}S^n)	n		$Y_0 \times 10^{-4}$ (Ω^{-1}cm^{-2}S^n)	n			
Bare	-	-	-	-	9.28	0.66	887	887	0.00006
Ni-P	0	8.41	0.90	90.09	4.96	0.67	1063	1153.09	0.00038
	25	7.50	0.90	111.9	4.18	0.68	1198	1309.90	0.00012
	50	6.03	0.90	120.2	4.05	0.72	1774	1894.20	0.00036
	75	5.24	0.92	167.8	3.00	0.76	2042	2209.80	0.00034
	100	8.27	0.85	56.27	6.53	0.62	1760	1816.27	0.00037
	150	9.06	0.64	20.62	5.22	0.67	1175	1195.62	0.00013
Ni-P-ND	0	12.25	0.83	71.43	15.62	0.64	1269	1340.43	0.00051
	25	12.06	0.85	76.41	4.36	0.70	1527	1603.41	0.00052
	50	9.24	0.85	79.69	5.54	0.72	1660	1739.69	0.00032
	75	15.31	0.87	42.87	19.99	0.84	2223	2265.87	0.00027
	100	17.83	0.82	35.23	8.11	0.77	1900	1935.23	0.00061
	150	1604	0.88	52.35	4.25	0.56	1161	1213.35	0.00022

Table 2. Potentiodynamic polarization parameters obtained for electroless Ni-P and Ni-P-ND coatings prepared without ultrasound and under ultrasonic agitation with the frequency of 75 kHz.

Sample	Ultrasound frequency (kHz)	E_{corr} (mV vs. Ag/AgCl)	i_{corr} (μA/cm^2)	b_a (mV/dec)	b_c (mV/dec)	R_p (kΩ cm^2)
Bare	-	-480.38	13.63	82.19	178.53	1.79
Ni-P	0	-472.70	10.12	95.10	117.76	2.25
	75	-414.45	6.44	94.62	94.59	3.18
Ni-P-ND	0	-518.77	7.87	76.94	156.32	2.84
	75	-488.61	5.24	64.64	127.46	3.55

To verify such a claim, the microhardness magnitudes of the Ni-P and Ni-P-ND coatings prepared under ultrasonic agitation with 75 kHz frequency were compared. Accordingly, the microhardness of the Ni-P coating increased from 578.0 to 644.2 HV$_{50}$ after the addition of ND particles. Moreover, the presence of nanoparticles reduces the possibility of creating cracks and porosity in the resulting coating. Table 1 indicates that the corrosion resistance of the two coatings enhanced as the deposition process was performed under ultrasonic agitation. Furthermore, the variation of ultrasound frequency was demonstrated to affect the surface properties of the deposited coatings. The corrosion resistance of the coatings increased with increasing the ultrasound wave frequency from 25 to 75 kHz but then reduced at higher frequencies. For instance, the polarization resistance ($R_p = R_{coat} + R_{ct}$) of the Ni-P-ND coating improved from 1340 $\Omega \cdot$cm^2 at the condition without ultrasound power to 2266 $\Omega \cdot$cm^2 under ultrasonic waves with the optimum frequency (75 kHz). The variation tendency in the values of n reported in Table 1 also needs to be considered. This parameter is an indication of the uniformity and smoothness of the surface. It is found that for both of the coatings, n increased with increasing the ultrasound frequency from 0 to 75 kHz and then decreased at higher frequencies. This observation indicates that imposing ultrasonic agitation in an optimum frequency during the deposition process could result in a smoother surface via
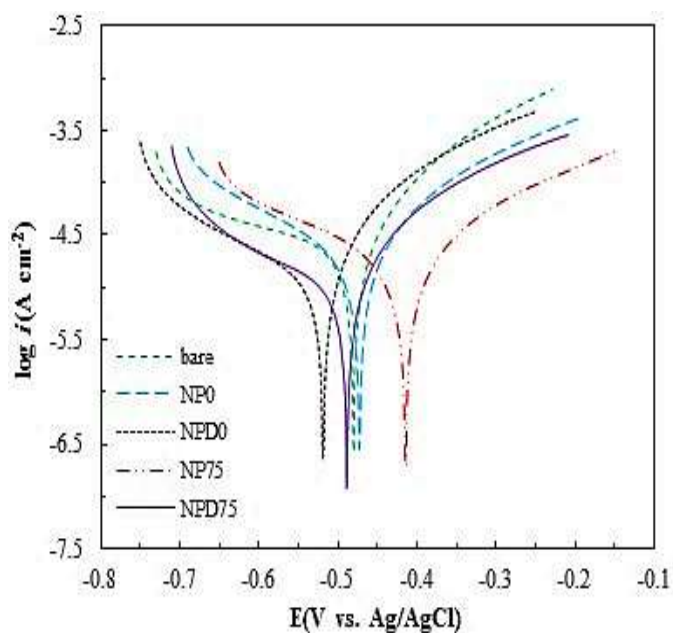
Fig. 5. Tafel plots measured for the electroless Ni-P and Ni-P-ND coatings produced under ultrasound with the frequency of 75 kHz (NP75 and NPD75) and without ultrasound (NP0 and NP75).

impeding the agglomeration of particles.

Further analysis concerning the corrosion performance of the synthesized coatings was carried out utilizing potentiodynamic polarization tests. The polarization curves of the Ni-P and Ni-P-ND coatings deposited under ultrasonic agitation with the optimum frequency were measured and compared to the bare steel. The obtained Tafel plots depicted in Fig. 5 were analyzed to obtain some parameters, such as corrosion potential (E_{corr}), corrosion current density (i_{corr}), and Tafel slopes (b_a and b_c), which are given in Table 2. Compared to the bare steel, all the coated samples exhibit better performance. This means a reduction in the corrosion current densities of the coated steel. This result indicates that the deposited coatings have successfully protected the metallic substrate from corrosion. Data included in Table 2 show that the coatings deposited under 75 kH ultrasound exhibit lower corrosion current densities. This observation is supported by the values of polarization resistance (R_p), where R_p values of Ni-P and Ni-P-ND layers deposited at the frequency 75 kH are higher than those of the same layers prepared without ultrasound. An inspection of Tafel slopes reveals that anodic slopes vary in a narrow range, whereas cathodic slopes show a significant change in the presence of coatings. This could mean that the protection of steel happens mainly by mitigation in the cathodic half-reaction.

4. Conclusion

Because of enhancing the corrosion protection properties of already reported Ni-P and Ni-P-ND coatings, various ultrasound frequencies were applied to agitate the plating bath to fabricate the mentioned coatings on mild steel. The characteristics of the prepared coatings were compared to those produced without ultrasound. In the case of coatings synthesized under ultrasonic power, the surface was smoother, as shown by the SEM images. The results from corrosion experiments suggested that the coatings of both types that were produced under ultrasound with 75 kHz frequency exhibited a remarkable improvement in their corrosion resistance.

References

[1] S. Chen, T. Liang, N. Wen, F.-H. Liu, C.-C. Tsao, C.-Y. Hsu, Electro-less plating nickel-phosphorus of low carbon steel using various pretreatments and an external magnetic field, J. Saudi Chem. Soc. 24 (2020) 704–714.

[2] F.-B. Wu, J.-G. Duh, Mechanical properties of sputtered nickel–phosphorus-based hard coatings under thermal annealing, Surf. Coatings Technol. 188 (2004) 500–505.

[3] J. Mashhadizadeh, A. Bozorgian, A. Azimi, Investigation of the kinetics of formation of Clatrit-like dual hydrates TBAC in the presence of CTAB, *Eurasian Chemical Communication,* 2 (2020), 536-547.

[4] I.A. Shozib, A. Ahmad, M.S.A. Rahaman, A. majdi Abdul-Rani, M.A. Alam, M. Beheshti, I. Taufiqurrahman, Modelling and optimization of microhardness of electroless Ni–P–TiO2 composite coating based on machine learning approaches and RSM, J. Mater. Res. Technol. 12 (2021) 1010–1025.

[5] B. Ghanavati, A. Bozorgian, Removal of Copper II from Industrial Effluent with Beta Zeolite Nanocrystals, *Progress in Chemical and Biochemical Research*, 5 (2022) 53-67.

[6] G. Zhao, R. Wang, S. Liu, T. Wang, D. Wu, Y. Zhang, J. Chen, Y. Zou, Microstructure analysis of element W in improving the Ni–P deposit thermal stability, J. Mater. Res. Technol. 9 (2020) 5474–5486.

[7] S. Karmalkar, R. Marjorie, V.G. Sumithra, Adhesion of electroless nickel plating on polished silicon, J. Adhes. Sci. Technol. 16 (2002) 1501–1507.

[8] C.-S. Chang, K.-H. Hou, M.-D. Ger, C.-K. Chung, J.-F. Lin, Effects of annealing temperature on microstructure, surface roughness, mechanical and tribological properties of Ni–P and Ni–P/SiC films, Surf. Coatings Technol. 288 (2016) 135–143.

[9] I.K. Hong, H. Kim, S.B. Lee, Optimization of barrel plating process for electroless Ni–P plating, J. Ind. Eng. Chem. 20 (2014) 3767–3774.

[10] M. Bagheri Sadr, A. Bozorgian, An Overview of Gas Overflow in Gaseous Hydrates, *Journal of Chemical Reviews*, 3 (2021), 66-82..

[11] B. Ghanavati, A. Bozorgian, J. Ghanavati, Removal of Copper (II) Ions from the Effluent by Carbon Nanotubes Modified with Tetrahydrofuran, *Chemical Review and Letters*, 5 (2022) 68-75.

[12] D.R. Dhakal, Y.K. Kshetri, G. Gyawali, T.-H. Kim, J.-H. Choi, S.W. Lee, Understanding the effect of Si3N4 nanoparticles on wear resistance behavior of electroless Nickel-Phosphorus coating through structural investigation, Appl. Surf. Sci. 541 (2021) 148403.

[13] J. Chen, Q. Meng, S. Zhang, K. Chong, W. Zhao, Y. Zou, Insights into corrosion resistance enhancement of nickel–phosphorus metallic glass in acid environment by the incorporation of copper, Vacuum. 195 (2022) 110705.

[14] J.T.W. Jappes, N.C. Brintha, M.A. Khan, N.J. Christo, Effect of modified method of coating on particle incorporation and wear resistance of nickel–phosphorus–diamond composite coatings, Mater. Today Proc. 45 (2021) 1509–1513.

[15] A. Ahmadpour, A. Bozorgian, A. Eslamimanesh, AH. Mohammadi, Photocatalytic treatment of spontaneous petrochemical effluents by TiO2 CTAB synthetic nanoparticles, *Desalination and Water Treatment*, 249 (2022) 297-308.

[16] A. Haghighi Asl, A. Ahmadpour, N. Fallah., Synthesis of Nano N-TiO2 for modeling of petrochemical industries spent caustic wastewater photocalitic treatment in visible light using DOE method, Applied Chemistry 12 (2017) 253-286.

[17] R. Hu, Y. Su, H. Liu, J. Cheng, X. Yang, Z. Shao, The effect of adding corrosion inhibitors into an electroless nickel plating bath for magnesium alloys, J. Mater. Eng. Perform. 25 (2016) 4530–4536.

[18] M. Islam, M.R. Azhar, Y. Khalid, R. Khan, H.S. Abdo, M.A. Dar, O.R. Oloyede, T.D. Burleigh, Electroless Ni-P/SiC nanocomposite coatings with small amounts of SiC nanoparticles for superior corrosion resistance and hardness, J. Mater. Eng. Perform. 24 (2015) 4835–4843.

[19] C. Zhao, Y. Yao, Preparation and mechanical properties of electroless nickel-phosphorus-tungsten carbide nanocomposite coatings, J. Mater. Eng. Perform. 23 (2014) 193–197.

[20] A. Bozorgian, Investigation of the effect of Zinc Oxide Nano-particles and Cationic Surfactants on Carbon Dioxide Storage capacity, *Advanced Journal of Chemistry, Section B: Natural Products and Medical Chemistry,* 3 (2021), 54-61.

[21] A.P. Meshram, M.K.P. Kumar, C. Srivastava, Enhancement in the corrosion resistance behaviour of amorphous NiP coatings by incorporation of graphene, Diam. Relat. Mater. 105 (2020) 107795.

[22] Z. Rajabalizadeh, D. Seifzadeh, A. Khodayari, S. Sohrabnezhad, Corrosion protection and mechanical properties of the electroless Ni-P-MOF nanocomposite coating on AM60B magnesium alloy, J. Magnes. Alloy. (2021).

[23] M.H. Sliem, K. Shahzad, V.N. Sivaprasad, R.A. Shakoor, A.M. Abdullah, O. Fayyaz, R. Kahraman, M.A. Umer, Enhanced mechanical and corrosion protection properties of pulse electrodeposited NiP-ZrO2 nanocomposite coatings, Surf. Coatings Technol. 403 (2020) 126340.

[24] A. Bozorgian, B. Raei, Thermodynamic Modeling and Phase Prediction for Binary System Dinitrogen Monoxide and Propane, *Journal of Chemistry Letters*, 1 (2021), 143-148.

[25] M. Sheng, C. Lv, L. Hong, M. Shao, K. Wan, F. Lv, The influence of ultrasonic frequency on the properties of Ni-Co coatings prepared by ultrasound-assisted electrodeposition, Acta Metall. Sin. (English Lett. 26 (2013) 735–741.

[26] L. Bonin, N. Bains, V. Vitry, A.J. Cobley, Electroless deposition of nickel-boron coatings using low frequency ultrasonic agitation: Effect of ultrasonic frequency on the coatings, Ultrasonics. 77 (2017) 61–68.

[27] I.R. Mafi, C. Dehghanian, Studying the effects of the addition of TiN nanoparticles to Ni–P electroless coatings, Appl. Surf. Sci. 258 (2011) 1876–1880.

[28] H. Luo, M. Leitch, Y. Behnamian, Y. Ma, H. Zeng, J.-L. Luo, Development of electroless Ni–P/nano-WC composite coatings and investigation on its properties, Surf. Coatings Technol. 277 (2015) 99–106.